HHS Public Access

Author manuscript

Nat Genet. Author manuscript; available in PMC 2014 June 01.

Published in final edited form as:

Nat Genet. 2013 December ; 45(12): 1428–1430. doi:10.1038/ng.2800.

Frequent truncating mutations of STAG2 in bladder cancer

David A. Solomon[1,2], **Jung-Sik Kim**[1], **Jolanta Bondaruk**[3], **Shahrokh F. Shariat**[4,5], **Zeng-Feng Wang**[6], **Abdel G. Elkahloun**[7], **Tomoko Ozawa**[8], **Julia Gerard**[1], **DaZhong Zhuang**[4], **Shizhen Zhang**[3], **Neema Navai**[9], **Arleen Siefker-Radtker**[10], **Joanna J. Phillips**[2], **Brian D. Robinson**[4,11], **Mark A. Rubin**[4,11], **Björn Volkmer**[12], **Richard Hautmann**[13], **Rainer Küfer**[14], **Pancras C. W. Hogendoorn**[15], **George Netto**[16], **Dan Theodorescu**[17], **C. David James**[8], **Bogdan Czerniak**[3], **Markku Miettinen**[6], and **Todd Waldman**[1]

[1]Department of Oncology, Lombardi Comprehensive Cancer Center, Georgetown University School of Medicine, Washington, DC, 20057, USA [2]Department of Pathology, University of California San Francisco, San Francisco, CA, 94143, USA [3]Department of Pathology, University of Texas MD Anderson Cancer Center, Houston, TX, 77030, USA [4]Department of Urology, Weill Cornell College of Medicine, New York, NY, 10065, USA [5]Division of Medical Oncology, Weill Cornell College of Medicine, New York, NY, 10065, USA [6]Laboratory of Pathology, National Cancer Institute, Bethesda, MD, 20892, USA [7]Cancer Genetics Branch, National Human Genome Research Institute, Bethesda, MD 20892, USA [8]Department of Neurological Surgery, University of California San Francisco, San Francisco, CA, 94143, USA [9]Department of Urology, University of Texas MD Anderson Cancer Center, Houston, TX, 77030, USA [10]Genitourinary Medical Oncology, University of Texas MD Anderson Cancer Center, Houston, TX, 77030, USA [11]Department of Pathology, Weill Cornell College of Medicine, New York, NY, 10065, USA [12]Department of Urology, Hospital Kassel, Kassel, Germany [13]Department of Urology, University Hospital Ulm, Ulm, Germany [14]Department of Urology, Hospital Am Eichert, Göppingen, Germany [15]Department of Pathology, Leiden University Medical Center, Leiden, Netherlands [16]Department of Pathology, Johns Hopkins University School of Medicine, Baltimore, MD, 21287, USA [17]Department of Surgery, University of Colorado Cancer Center, University of Colorado School of Medicine, Aurora, CO, 80045, USA

Abstract

Here we report the discovery of truncating mutations of the gene encoding the cohesin subunit STAG2, which regulates sister chromatid cohesion and segregation, in 36% of papillary non-invasive urothelial carcinomas and 16% of invasive urothelial carcinomas of the bladder. Our studies suggest that STAG2 plays a role in controlling chromosome number but not proliferation

Correspondence should be addressed to Todd Waldman (waldmant@georgetown.edu).

AUTHOR CONTRIBUTIONS

D.A.S., J.S.K., J.B., S.F.S., C.D.J., B.C., M.M., and T.W. designed research; D.A.S., J.S.K., J.B., Z.F.W., A.G.E., T.O., J.G., D.Z., S.Z., and J.J.P. performed research; J.B., S.F.S., D.Z., M.A.R., B.V., R.H., R.K., P.C.H., G.N., D.T., B.C., and M.M. contributed new reagents/analytic tools; D.A.S., J.S.K., S.F.S., A.G.E., N.N., A.S.R., B.D.R., C.D.J., M.M., and T.W. analyzed data; D.A.S., S.F.S., and T.W. wrote the paper.

of bladder cancer cells. These findings identify STAG2 as among the most commonly mutated genes in bladder cancer discovered to date.

Inactivating mutations of the cohesin complex gene STAG2 have recently been identified in human cancer and were demonstrated to cause chromosome segregation defects and aneuploidy[1,2,3]. To identify additional tumor types with inactivation of the STAG2 gene, we screened 2,214 human tumors by immunohistochemistry (IHC) using a STAG2 monoclonal antibody that binds at the carboxyl terminus of the protein. As the STAG2 gene is on the X chromosome, complete genetic inactivation of STAG2 requires only a single mutational event. Virtually all tumor-derived STAG2 mutations discovered to date are truncating (*e.g.* nonsense, frameshift, splice-site) which lead to absence of the carboxyl-terminal epitope and therefore loss of expression via IHC with this antibody[1]. STAG2 was robustly expressed specifically in the nucleus in all non-neoplastic tissues studied (examples in Supplementary Figures 1–2).

We discovered that 52/295 urothelial carcinomas of the bladder (18%) had complete loss of STAG2 expression (Supplementary Table 1 and Supplementary Figure 3). Occasional loss of STAG2 expression was also identified in several other tumor types (Supplementary Figures 4–6). Urothelial carcinomas staining negatively for STAG2 included a wide range of stages and grades, from low-grade, non-invasive papillary tumors to high-grade, muscle invasive tumors. In each case with STAG2 loss, non-neoplastic stroma and endothelial cells retained expression, demonstrating the somatic nature of STAG2 loss in these tumors. STAG2-negative bladder tumors stained positively with antibodies to the constitutively expressed nuclear protein Ini-1, demonstrating intact immunoreactivity for other nuclear antigens (Supplementary Figure 7). In the vast majority of cases, all tumor cells were negative for STAG2 expression; however, in a small number of cases (2/52), there was evidence of mosaicisim (*i.e.* intratumoral heterogeneity) wherein some regions of the tumor retained expression of STAG2 (Supplementary Figure 8). Whereas tumors with complete loss suggests that STAG2 inactivation occurred as an early initiating event in these cases, the small number of mosaic tumors suggests that STAG2 can occasionally be inactivated during the early progression stage of urothelial tumorigenesis.

To determine the mechanism of STAG2 loss, we used Sanger sequencing to analyze the STAG2 gene in genomic DNA purified from an independent cohort of 111 primary urothelial carcinomas of various grades and stages (clinicopathologic characteristics in Supplementary Table 2). 25 mutations were identified in 23 of the cases, with two samples harboring two independent mutations each (Figure 1A and Supplementary Table 3). Apart from known SNPs, no synonymous mutations were identified. 21/25 mutations resulted in premature truncation of the encoded protein including 5 nonsense, 6 splice site, and 10 frameshift mutations (Supplementary Figure 9). All mutations were shown to be somatic in samples with matched constitutional DNA (8 samples; Supplementary Table 3). Mutations were identified in 9/25 (36%) of pTa non-invasive papillary carcinomas, 6/22 (27%) of pT1 superficially invasive carcinomas, and 8/64 (13%) of pT2-T4 muscle invasive carcinomas. Tumors with truncating STAG2 mutations were negative for STAG2 expression via IHC (examples in Figure 1B and Supplementary Figure 10). Tumors with missense mutations

retained expression of STAG2 by IHC, demonstrating that IHC fails to identify the ~15% of STAG2-mutant tumors with missense mutations of the gene (Supplementary Figure 11). Truncating mutations were also observed in 5/32 urothelial carcinoma cell lines (Supplementary Figure 12). Tumors and cell lines with STAG2 mutation frequently had concurrent p53 overexpression or mutation (Supplementary Figure 13 and Supplementary Table 3).

Next we performed molecular cytogenetic analysis on 12 primary urothelial carcinomas with STAG2 mutations and 12 stage-matched tumors with wild-type STAG2. Genomic DNA was interrogated using Affymetrix CytoScan HD Arrays and chromosomal gains and losses were scored for each sample (Supplementary Table 4 and Supplementary Figures 14–15). 9/12 STAG2 mutant tumors studied were overtly aneuploid with up to 35 clonal chromosomal aberrations in a single tumor, whereas 3 tumors with STAG2 mutations did not contain detectable chromosomal aberrations. 10/12 tumors with wild-type STAG2 also contained chromosomal copy number aberrations, demonstrating that there are other pathways whose perturbation also leads to aneuploidy in bladder cancer.

We then constructed a STAG2-expressing lentivirus and infected UM-UC-3, UM-UC-14, and VM-CUB-3 cells, three urothelial carcinoma cell lines with truncating mutations of STAG2 (Figure 2A and Supplementary Figure 16). Ectopic re-expression of STAG2 had no adverse effect on cellular proliferation or *in vivo* growth as subcutaneous xenografts (Figure 2B and Supplementary Figure 16). Ectopic re-expression of STAG2 did not overtly reduce the degree of aneuploidy (Supplementary Figure 17), perhaps because once aneuploidy is established it is thought to be largely self-sustaining. In contrast, depletion of wild-type STAG2 via lentiviral shRNA led to a distinct alteration in the modal chromosome number of RT4 urothelial carcinoma cells (Figure 2C–D and Supplementary Figure 18). Taken together, these functional experiments provide support for the hypothesis that STAG2 may play a role in controlling chromosomal stability but not cellular proliferation of bladder cancer cells.

We next determined the STAG2 status of a panel of 34 papillary non-muscle invasive urothelial carcinomas treated with transurethral resection with a median follow-up of 54 months (clinicopathologic features in Supplementary Table 5). In this cohort, STAG2 loss was significantly associated with increased disease-free survival (Supplementary Figure 19; p=0.05). Only 1/8 (12%) of the STAG2-deficient carcinomas recurred (as a non-invasive carcinoma), whereas 15/26 (58%) of the STAG2-expressing carcinomas recurred (two which recurred as invasive carcinomas and four of which metastasized).

We then determined the STAG2 status of a clinically annotated panel of 349 invasive urothelial carcinomas treated with radical cystectomy with a median follow-up of 130 months (clinicopathologic features in Supplementary Table 6). In these invasive tumors, STAG2 loss was significantly associated with increased frequency of lymph node metastasis (p=0.03). IHC analysis of paired primary tumors and lymph node metastases demonstrated that STAG2 loss was present in the primary tumor before lymphovascular invasion occurred (Supplementary Figure 20). Loss of STAG2 expression was also associated with increased risk of disease recurrence (p=0.04) and cancer-specific mortality (p=0.04; Supplementary

Figure 21). The biological basis for the different effects of STAG2 status on the clinical outcome of non-muscle invasive papillary carcinomas versus muscle invasive carcinomas is currently unknown.

Bladder cancer is the fifth most common human malignancy in the United States, with approximately 74,000 new cases diagnosed per year and approximately 15,000 deaths[4]. Bladder cancer is thought to arise via two different pathways - from papillary lesions which frequently recur but only 15–20% of which progress to muscle invasion, and from flat dysplastic lesions (carcinoma in situ) which directly progress to muscle invasion without a papillary precursor lesion. The majority of bladder cancers are papillary non-invasive tumors; clinical management of these tumors poses a serious dilemma since it is currently not possible to prospectively identify those which will recur or progress to invasion.

It is notable that STAG2 mutations occur and are most common in early stage bladder cancers including non-invasive papillary carcinomas. As such, we conclude that STAG2 mutation is an early event in bladder tumorigenesis. Furthermore, we find that the major mechanism for STAG2 inactivation in bladder cancer is somatic nonsense (~85%) and missense (~15%) mutations (rather than homozygous deletion or promoter hypermethylation), since all STAG2-deficient cell lines and primary tumors studied harbor truncating mutations in the gene.

Whether mutations in STAG2 are a direct cause of aneuploidy in human cancer is currently a source of controversy because a subset of STAG2-deficient acute myeloid leukemias and urothelial carcinomas appear to be diploid (refs. 2, 5 and Supplementary Table 4). Despite these surprising observations, there are several lines of evidence supporting a direct role for STAG2 inactivation as a cause of aneuploidy in cancer. In yeast, mutation of cohesin complex genes causes aberrant chromosome segregation and aneuploidy[6,7]. Recently, a mouse harboring genetic inactivation of STAG1, a homolog of STAG2, was generated which displays increased aneuploidy due to chromosome segregation defects[8]. Targeted inactivation of STAG2 in HCT116 colon cancer cells and depletion of STAG2 in RT4 bladder cancer cells leads to alterations in modal chromosome number (ref. 1 and Figure 2D). Also, ectopic expression of STAG2 has no adverse effect on cellular proliferation or *in vivo* growth (Figure 2B and Supplementary Figure 16), and targeted correction of endogenous mutant STAG2 in two cancer cell lines resulted in no significant change in global gene expression profiles, arguing against a role for STAG2 in controlling signaling pathways, cellular proliferation, apoptosis, or other transformation-associated processes[1].

Finally, this discovery has potentially important clinical applications, since a major problem in the treatment of bladder cancer has been the identification of those 15–20% of papillary tumors which will recur and progress to invasion versus the 80–85% which will not. Here we report that STAG2 is mutationally inactivated in greater than one third of papillary non-invasive bladder tumors, and that these tumors with STAG2 loss rarely recur or progress, perhaps explaining the difference in the frequencies of STAG2 inactivation in non-invasive urothelial carcinomas (36%) compared to that in invasive urothelial carcinomas (16%). As the immunohistochemical assay for STAG2 loss is robust and routine clinical sequencing of

tumors is imminent, the discovery reported here may have near-term implications for the clinical management of patients with bladder cancer.

ONLINE METHODS

Tumor Specimens

1,848 of the 2,214 tumor samples screened by immunohistochemistry and described in Supplementary Table 1 were anonymized, well characterized tumor samples assembled into multi-tumor blocks containing 5–50 cases each, as described previously[9,10]. The remainder of the 366 samples described in Supplementary Table 1 were from: (i) a Ewing's sarcoma TMA created from resection specimens at Leiden University Medical Center containing 21 informative cases spotted in triplicate, (ii) ovarian cancer TMA OV1921 from US Biomax containing 76 informative cases spotted in duplicate, (iii) bladder cancer TMA BL1002 from US Biomax containing 37 informative cases spotted in duplicate, (iv) bladder cancer TMA BLC1501 from US Biomax containing 70 informative cases spotted in duplicate; (v) bladder cancer TMA BL1921 from US Biomax containing 79 informative cases spotted in duplicate; and (vi) a bladder cancer TMA created from resection specimens at the MD Anderson Cancer Center containing 83 informative cases[11].

For DNA sequencing, genomic DNA was prepared from snap-frozen, treatment-naïve urothelial carcinomas resected at the MD Anderson Cancer Center and the Johns Hopkins University Hospital. The clinicopathological characteristics of these tumors are described in Supplementary Table 2.

For the outcomes study described in Supplementary Figure 19, a clinically annotated TMA containing 34 cases of papillary non-muscle invasive urothelial carcinoma of the bladder from patients treated with transurethral resection was assessed for STAG2 status by immunohistochemistry. The creation and validation of this TMA has been described previously[11].

For the outcomes study described in Supplementary Figure 21, a clinically annotated TMA created from 349 consecutive patients treated with radical cystectomy for invasive urothelial carcinoma of the bladder between 1988 and 2003 at a single center was assessed for STAG2 status by immunohistochemistry. The creation and validation of these TMAs has been described previously[12]. No patient received preoperative systemic chemotherapy or radiotherapy, and no patient had known metastatic disease at the time of surgery. Postoperatively, patients were generally seen at least three times in year 1, semiannually in year 2, and annually thereafter. Diagnostic imaging of the upper tract and chest radiography were performed at least annually, or as clinically indicated. Patients identified as having died of urothelial carcinoma had progressive, disseminated and often symptomatic metastases at death.

Immunohistochemistry

A STAG2 mouse monoclonal antibody from Santa Cruz Biotechnology (clone J-12, sc-81852) was used at a dilution of 1:100. A p53 mouse monoclonal antibody from Dako (clone DO-7, #M7001) was used at a 1:25 dilution. Immunostaining was performed in an

automated immunostainer (Leica Bond-Max) following heat-induced antigen retrieval for 30 min in high pH epitope retrieval buffer (Bond-Max). Primary antibody was applied for 30 min, followed by Bond-Max polymer for 15 min. Diaminobenzidine was used as the chromogen, followed by hematoxylin counterstain. Samples in which both the tumor cells and normal cells failed to stain for STAG2 were considered antigenically non-viable and were excluded from the analysis.

DNA sequencing

Individual exons of STAG2 were PCR amplified from genomic DNA using conditions and primer pairs described by Solomon *et al.*[1] PCR products were purified using the Exo/SAP method followed by a Sephadex spin column. Sequencing reactions were performed using Big Dye v3.1 (Applied Biosystems) using an M13F primer, and analyzed on an Applied Biosystems 3730XL capillary sequencer. Sequences were analyzed using Mutation Surveyor (Softgenetics). Traces with putative mutations were re-amplified and sequenced from both tumor and matched normal DNA from blood when available.

Western blot

Primary antibodies used were STAG2 clone J-12 (Santa Cruz Biotechnology, sc-81852) and α-tubulin Ab-2 clone DM1A (Neomarkers). Protein was isolated from 32 human urothelial carcinoma cell lines in RIPA buffer, resolved by SDS-PAGE, and immunoblotted following standard biochemical techniques.

Molecular cytogenetics

Genomic DNA purified from 24 snap-frozen primary urothelial carcinomas was interrogated with Affymetrix CytoScan HD Arrays according to the manufacturer's instructions. The scanned array images and processed data sets have been deposited in the Gene Expression Omnibus (http://www.ncbi.nlm.nih.gov/geo, dataset GSE41581)..CEL files were generated from the scanned array image files by the Affymetrix GeneChip Command Console Software and were imported into the Affymetrix Chromosome Analysis Suite v1.2.2 Software. Copy number data files (.CYCHP files) were generated using the ChAS Analysis Files for the CytoScan HD Array version NA32.1 (hg19) as a reference.

STAG2 lentiviral expression and shRNA depletion

To create a STAG2-expressing lentivirus, a human STAG2 cDNA corresponding to CCDS14607 was synthesized (Genscript) and cloned into the lentiviral expression vectors pHR-SIN (a gift from Nick Leslie) and pLJM1 (Addgene), and packaged by co-transfection of 293T cells with lentiviral helper plasmids pHR′CMV8.2ΔR and pCMV-VSV-G as previously described[13]. Virus-containing conditioned medium was harvested 48 hrs after transfection, filtered, and used to infect recipient cells in the presence of 8 μg/mL polybrene. Infected cells were selected with 2 μg/mL puromycin until all mock-infected cells were dead and then maintained in puromycin. The identification and validation of lentiviral STAG2 shRNA constructs have been previously described[5].

CellTiter-Glo proliferation assay

Proliferation of pooled clones of STAG2 mutant urothelial cancer cells infected with lentiviral-vector or lentiviral-STAG2 was performed using CellTiter-Glo Luminescent Cell Proliferation Assay according to the manufacturer's instructions (Promega).

Subcutaneous xenograft growth assay

Three million cells from pooled clones of UM-UC-3 cells infected with either lentiviral-empty vector or lentiviral-STAG2 following puromycin selection were injected subcutaneously into the flanks of 5 to 6 week old female athymic mice (nu/nu genotype, BALB/c background; Simonsen Laboratories). Tumor volume was measured three times weekly starting at day thirteen post-injection. Animals were housed and fed under aseptic conditions, and all animal research was approved by The University of California, San Francisco Institutional Animal Care and Use Committee.

Chromosome counting

Cultured cells were treated with 0.02 μg/ml colcemid for 55 minutes at 37°C. The cells were then trypsinized, centrifuged for 7 minutes at 200×g, and the cell pellet resuspended in warmed hypotonic solution and incubated at 37°C for 11 minutes. The swollen cells were then centrifuged and the pellet resuspended in 8 mL of Carnoy's fixative (3:1 methanol:glacial acetic acid). After incubation in fixative at room temperature for 96 minutes, the cell suspension was centrifuged and washed twice in Carnoy's fixative. After the last centrifugation, the cells were resuspended in 1 to 3 mL of freshly prepared fixative to produce an opalescent cell suspension. Drops of the final cell suspension were placed on clean slides and air-dried. Slides were stained with a 1:3 mixture of Wright's stain and 0.06 M phosphate buffer for 4–10 minutes, washed with tap water for 5 seconds, and then air-dried. One hundred cells in metaphase were examined for chromosome count in a blinded fashion.

Statistical analysis

Analyses were performed with SPSS® 17 (SPSS Inc., IBM Corp.). Differences in variables with a continuous distribution across categories were assessed using the Mann-Whitney U test (two categories) and Kruskal-Wallis test (three and more categories). The Fisher's exact test and the chi-square ($\chi 2$) test were used to evaluate the association between categorical variables. Univariable recurrence and cancer-specific survival probabilities were estimated using the Kaplan-Meier method and differences assessed using the log-rank test. All tests are two-sided and a p-value of 0.05 was set to be statistically significant.

Supplementary Material

Refer to Web version on PubMed Central for supplementary material.

ACKNOWLEDGEMENTS

We thank Bert Vogelstein for assistance in acquiring samples and preparing genomic DNA. This work was supported by NIH grants R01CA169345, R01CA159467, and R21CA143282 to T.W., and the MD Anderson Cancer Center Bladder Cancer SPORE grant P50CA091846.

A provisional patent application has been filed by Georgetown University related to the technology described in this paper, on which Drs. Solomon, Kim, and Waldman are the inventors.

References

1. Solomon DA, et al. Science. 2011; 333:1039–1043. [PubMed: 21852505]
2. Walter MJ, et al. N. Engl. J. Med. 2012; 366:1090–1098. [PubMed: 22417201]
3. Cancer Genome Atlas Research Network. Nature. 2011; 474:609–615. [PubMed: 21720365]
4. Howlader, N., et al., editors. SEER Cancer Statistics Review, 1975–2009 (Vintage 2009 Populations). http://seer.cancer.gov/csr/1975_2009_pops09/, based on November 2011 SEER data submission.
5. Welch JS, et al. Cell. 2012; 150:264–278. [PubMed: 22817890]
6. Michaelis C, Ciosk R, Nasmyth K. Cell. 1997; 91:35–45. [PubMed: 9335333]
7. Rao H, et al. Nature. 2001; 410:955–959. [PubMed: 11309624]
8. Remeseiro S, et al. EMBO J. 2012; 31:2076–2089. [PubMed: 22415365]
9. Miettinen M. Appl. Immunohistochem. 2012; 20:410–412.
10. Miettinen M, et al. Am. J. Surg. Pathol. 2012; 36:629–639. [PubMed: 22314185]
11. Kim JH, et al. Lab. Invest. 2005; 85:532–549. [PubMed: 15778693]
12. Rink M, et al. Urol. Oncol. 2012 Epub Sept 1,
13. Solomon DA, et al. Cancer Res. 2008; 68:10300–10306. [PubMed: 19074898]

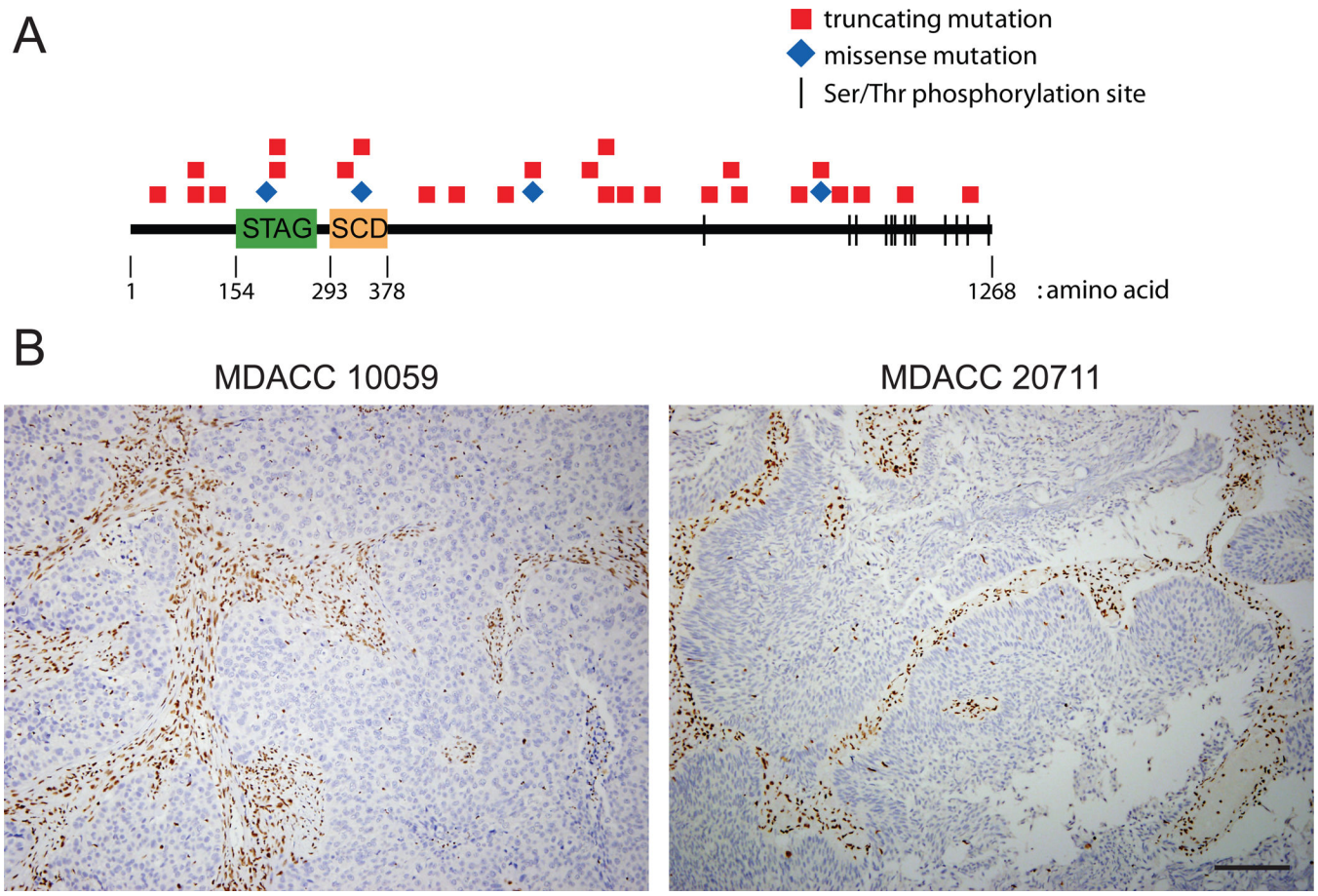

Figure 1.

Frequent truncating mutations of STAG2 in urothelial carcinoma of the bladder. (A) Diagram of STAG2 protein with location of mutations in urothelial carcinomas identified in this study. STAG, stromal antigen domain; SCD, stromalin conserved domain. (B) Examples of complete somatic loss of STAG2 expression by immunohistochemistry in two urothelial carcinomas harboring truncating mutations of STAG2 (nonsense mutation in MDACC 10059 and canonical splice acceptor mutation in MDACC 20711, see Supplementary Figure 10). There is retained expression within the non-neoplastic fibrovascular stroma in each case.

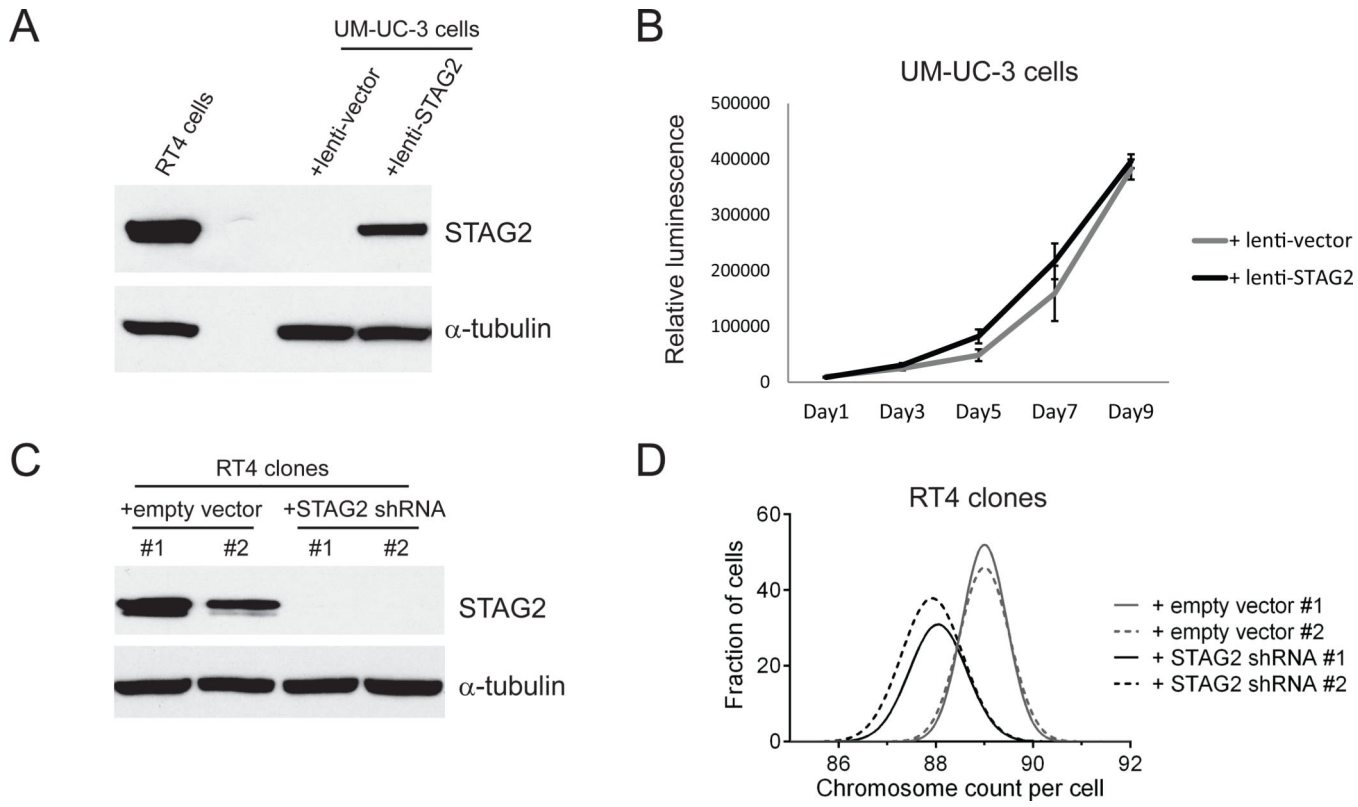

Figure 2.

Effects of STAG2 inactivation on proliferation and chromosomal stability in urothelial cancer cells. (A) Western blot demonstrating lentiviral re-expression of wild-type STAG2 in UM-UC-3 cells, which harbor an endogenous truncating mutation. The level of re-expression is comparable to the endogenous level of STAG2 protein in RT4 cells, which harbor a wild-type STAG2 gene. (B) Proliferation of UM-UC-3 pooled clones infected with either lentiviral-STAG2 or lentiviral-empty vector after five days of selection in puromycin, measured via CellTiter-Glo assay. (C) Western blot depicting expression of endogenous STAG2 in individual clones of RT4 cells following infection with either lentiviral-empty vector or lentiviral-STAG2 shRNA. (D) Gaussian distribution plots depicting chromosome numbers per cell in the individual RT4 cell clones depicted in C. Chromosome counts for 100 cells were determined in metaphase spreads for each clone. Individual chromosome numbers are listed in Supplementary Figure 18.